Ultrastructural Studies on Scrapie Prion Protein Crystals Obtained from Reverse Micellar Solutions

Holger Wille* and Stanley B. Prusiner*#
Departments of *Neurology and #Biochemistry and Biophysics, University of California, San Francisco, California 94143 USA

ABSTRACT The structural transition from the cellular prion protein (PrP^C) that is rich in α-helices to the pathological form (PrP^{Sc}) that has a high β-sheet content seems to be the fundamental event underlying the prion diseases. Determination of the structure of PrP^{Sc} and the N-terminally truncated PrP 27-30 has been complicated by their insolubility. Here we report the solubilization of PrP 27-30 through a system of reverse micelles that yields monomeric and dimeric PrP. Although solubilization of PrP 27-30 was not accompanied by any recognizable change in secondary structure as measured by FTIR spectroscopy, it did result in a loss of prion infectivity. The formation of small two- and three-dimensional crystals upon exposure to uranyl salts argues that soluble PrP 27-30 possesses considerable tertiary structure. The crystals of PrP 27-30 grown from reverse micellar solutions suggest a novel crystallization mechanism that might be applicable for other membrane proteins. A variety of different crystal lattices diffracted up to 1.85 nm by electron microscopy. Despite the lack of measurable biological activity, the structure of PrP 27-30 in these crystals may provide insight into the structural transition that occurs during PrP^{Sc} formation.

INTRODUCTION

Scrapie of sheep, bovine spongiform encephalopathy, and Creutzfeldt-Jakob disease of humans are all caused by PrP^{Sc} (Prusiner, 1997). Spectroscopic analysis has shown that PrP^C contains mostly α-helices and is almost devoid of β-sheet, whereas PrP^{Sc} and PrP 27-30, which is N-terminally truncated at approximately residue 90, are dominated by β-sheet structure (Caughey et al., 1991; Gasset et al., 1993; Pan et al., 1993; Prusiner et al., 1983; Safar et al., 1993). Replication of prions features a profound change in the conformation of PrP. Current hypotheses on the mechanism for nascent PrP^{Sc} formation include the template-assistance model (Cohen and Prusiner, 1998) and the seeded nucleation hypothesis (Gajdusek, 1988; Jarrett and Lansbury, 1993). Prion strain-specified information is enciphered in the conformation of PrP^{Sc}, arguing that PrP^{Sc} must act as a template in the formation of nascent PrP^{Sc} (Bessen and Marsh, 1994; Safar et al., 1998; Telling et al., 1996b).

The seeded nucleation hypothesis argues for a crystallization-like mechanism where seeds consisting of ordered polymers initiate polymerization. Despite the demonstration that PrP amyloid is neither necessary nor sufficient for infectivity (Gabizon et al., 1987; McKinley et al., 1991; Pan et al., 1993; Prusiner et al., 1990; Wille et al., 1996), proponents of seeded nucleation hypothesis persist (Caughey and Chesebro, 1997; Caughey et al., 1997). Although large polymeric structures can be excluded from being essential for prion formation, oligomers may serve as a template (for reviews see Cohen and Prusiner, 1998; Eigen, 1996; Harper and Lansbury, 1997; Harrison et al., 1997; Safar, 1996).

The scrapie agent's hydrophobic nature and propensity to aggregate impeded attempts to purify it (Millson et al., 1976; Prusiner et al., 1978). Multiple attempts to separate prion infectivity from membranes were unsuccessful (Hunter et al., 1968; Hunter and Millson, 1967; Malone et al., 1978; Marsh et al., 1984; Prusiner et al., 1980; Safar et al., 1991), in accord with the association of PrP^{Sc} with membranes. Because of difficulties in solubilizing, structural studies of both PrP^{Sc} and PrP 27-30 have been elusive. PrP 27-30 readily polymerizes into large rod-shaped aggregates with the tinctorial properties of amyloid (Prusiner et al., 1983), but the prion rods are an artifact of the purification procedure (McKinley et al., 1991). Although solubilization of purified PrP 27-30 using a combination of detergent and phospholipid to form DLPCs increased prion titers (Gabizon et al., 1987, 1988), DLPCs interfered with crystallization. Solubilization of PrP 27-30 with the denaturing detergent SDS, even at low concentrations, resulted in diminished prion infectivity (Prusiner et al., 1983; Riesner et al., 1996). Treatment of prion rods with 0.1% SDS and sonication produced spherical particles of ~10 nm in diam-

Received for publication 24 July 1998 and in final form 8 November 1998.

Address reprint requests to Dr. Stanley B. Prusiner, Department of Neurology, Box 0518, University of California, San Francisco, CA 94143-0518. Tel.: 415-476-4482; Fax: 415-476-8386.

Abbreviations used: PrP^{Sc}, pathological isoform of PrP; AOT, sodium bis(2-ethylhexyl)sulfosuccinate (=dioctylsulfosuccinate, sodium salt; =Aerosol OT); APFO, perfluorooctanoate, ammonium salt; CD, circular dichroism; DLPC, detergent-lipid-protein-complex; FTIR, Fourier transform infrared; GdnHCl, guanidine hydrochloride; HFIP, hexafluoro-2-propanol; HFPIP, 1,1,1,3,3,3-hexafluoro-2-phenyl-2-propanol; IEP, isoelectric point (of a protein); IR, infrared; isooctane, 2,2,4-trimethylpentane; LDAO, lauryldimethylamine oxide; NFBSA, nonafluorobutanesulfonic acid, potassium salt; PBSZ, phosphate buffered saline with zwittergent 3–12; PK, proteinase K; PMSF, phenylmethylsulfonyl fluoride; PrP, prion protein; PrP 27-30, PK-resistant C-terminal fragment of PrP^{Sc} (residues ~90 to 231); PrP^C, cellular isoform of PrP; RT, room temperature; $S_{20,w}$ value, Svedberg sedimentation coefficient normalized to 20°C and the viscosity of water; TFIP, 1,1,1-trifluoro-2-propanol.

0006-3495/99/02/1048/15 $2.00

eter that were unsuitable for crystallization (Riesner et al., 1996). Other reports showed little, if any, solubilization with the infectious prions migrating with a sedimentation coefficient of ~120 S (Akowitz et al., 1990; Kimberlin et al., 1971; Sklaviadis et al., 1992).

On this background, we initiated studies employing organic solvents in combination with a variety of nondenaturing detergents for solubilization of PrP 27-30 that was polymerized into prion rods. Through a process of liquid-liquid extraction via reverse micelles (Göklen and Hatton, 1987; Wolbert et al., 1989) and an organic phase, PrP 27-30 was solubilized into predominantly monomers and dimers. Although solubilization of PrP 27-30 was not accompanied by any recognizable change in secondary structure as measured by FTIR spectroscopy, it did result in a loss of prion infectivity. Small two- and three-dimensional crystals were formed upon exposure of soluble PrP 27-30 to uranyl salts directly from the reverse micellar solutions. This finding, as well as the preservation of secondary structure, argues that soluble PrP 27-30 possesses considerable tertiary structure. To our knowledge, this is the first time that a membrane or membrane-associated protein has been crystallized from reverse micelles. Electron microscopy showed multiple crystal forms, and electron diffraction revealed reflections up to 1.85 nm.

MATERIALS AND METHODS

Materials and solvents

The solvents and detergents used in this study were purchased from the following sources: AOT, Sigma, St. Louis, MO; APFO, Fluka Chemie, Buchs, Switzerland; HFIP, Aldrich, Milwaukee, WI; HFPIP, Aldrich; isooctane, Fluka Chemie; NFBSA, Aldrich; saponin, Calbiochem/Behring Diagnostics, La Jolla, CA; TFIP, Narchem, Chicago, IL. All solvents were of the highest purity commercially available. Salts and heavy metal compounds for negative staining and crystallization assays were obtained from the following sources: ammonium molybdate, Electron Microscopy Sciences, Fort Washington, PA; aurothioglucose, bismuth nitrate, bismuth oxynitrate, cadmium iodide, copper sulfate, lanthanum nitrate, lead acetate, and thallium acetate, Sigma; uranyl acetate, Fluka Chemie; uranyl formate, Polysciences, Warrington, PA; uranyl nitrate, Fluka Chemie; vanadylsulfate, SPI supplies, West Chester, PA; zinc sulfate, Sigma. All salts and negative staining compounds were of the highest purity commercially available.

Prion protein

PrP 27-30 was prepared as described previously (Prusiner et al., 1983). The last step of preparation included a sucrose gradient centrifugation in a zonal rotor. Before the solubilization assays, PrP 27-30 was precipitated out of the sucrose by dilution and an ultracentrifugation step (Beckman rotor SW28, 24,000 rpm, 4°C, 16 h). The protein pellet was resuspended in 50 mM NaHEPES, 0.5 mM NaN_3 pH 7.4 at a protein concentration of ~1 mg/ml or above and kept frozen until use.

Solubilization assay

PrP 27-30 was used mostly in concentrations ranging from 100 to ~500 μg/ml. Standard buffer was 50 mM NaHEPES, 1 mM PMSF, 0.5 mM NaN_3 pH 7.4 unless indicated otherwise. Detergents were used at concentrations of 5 to 10 times the critical micelle concentration (w/v) and organic solvents were added at concentrations up to and well above the limits of miscibility with aqueous buffers (v/v). Solubilization assays were incubated at 37°C for 4 h (shorter incubation periods proved to be less successful) with frequent agitation in order to keep PrP 27-30 in suspension and the multiple liquid phases mixed. The incubation was followed by an ultracentrifugation at 100,000 × g for 1 h (Beckman rotor TLA 45 43,000 rpm 20°C). After centrifugation, the samples were separated into supernatant and pellet; the supernatant could often be differentiated into an organic and an aqueous phase with or without particles at the interphase. Pellets were resuspended in 50 mM NaHEPES, 0.5 mM NaN_3 pH 7.4. Small aliquots of pellets and supernatants were used for SDS gel electrophoresis, bioassays, and negative stain electron microscopy. The remaining sample was stored at 4°C, and no substantial changes were observed during periods of up to 6 months, provided appropriate storage vials were used. Isooctane-containing samples required storage in glass vials because the solvent evaporated through the plastic walls of conventional tubes.

SDS-PAGE and Western blotting

SDS gel electrophoresis was performed with 15% polyacrylamide gels. The gels were blotted onto polyvinylidene difluoride membranes. Membranes were saturated with 5% nonfat dry milk in TBST (10 mM Tris HCl pH 8.0, 150 mM NaCl, 0.05% (v/v) Tween 20) for 1 h at RT. The α-PrP polyclonal antiserum (N10) was used at 1:4000 dilution in TBST in an overnight incubation at RT (H. Serban et al., manuscript in preparation). The primary antibody was detected by using a horseradish peroxidase-coupled secondary antibody and the ECL system (Amersham, Little Chelfont, Buckinghamshire, UK).

Bioassays

Bioassays were performed by inoculating 50-μl samples intracerebrally into weanling female hamsters (LVG/LAK) purchased from Charles River Laboratories. Samples were diluted 100-fold into phosphate buffered saline with 5 mg/ml bovine serum albumin as a carrier. Prion titers were determined by measuring the incubation time intervals from inoculation to the onset of neurological illness (Prusiner et al., 1980).

Negative stain electron microscopy, electron diffraction, and crystallization of PrP 27-30

Negative staining was done on carbon-coated 1000-mesh copper grids that were glow-discharged before staining. One- to 5-μl samples were adsorbed for up to 1 min, and all samples were then stained with freshly filtered 2% ammonium molybdate or 2% uranyl acetate. Dried samples were viewed in a Jeol 100CX II electron microscope at 80 kV at a standard magnification of 40,000. The magnification was calibrated using negatively stained catalase crystals and ferritin. Electron diffraction was done with a camera length of 2.4 m and a diffraction aperture of 0.3 μm, covering nonrelevant objects as much as possible. Exposure times for the electron diffractograms were in the order of minutes, practically destroying all high-resolution information. The length of the exposure time and the presence of uranyl ions within the crystal lattice limit the resolution practically to that of optical diffraction methods. Crystallization of PrP 27-30 was first observed after negative staining with 2% unbuffered uranyl acetate solution (pH ~3.8) while unbuffered 2% ammonium molybdate (pH ~5.4) yielded no such crystals. Buffered 2% ammonium molybdate, 50 mM sodium acetate pH 4.0 did not induce PrP 27-30 to crystallize, while the use of buffered uranyl acetate (2% uranyl acetate, 50 mM sodium acetate pH 4.0) improved the quality of the crystals. Unbuffered saturated uranyl formate (<1% uranyl formate, pH ~3.5) and unbuffered 2% uranyl nitrate (pH ~2.8) gave equally well-formed but smaller PrP 27-30 crystals. A large number of other salts and negative stain agents were tested, but none induced the formation of PrP 27-30 crystals (see Results).

Dynamic light scattering

Hydrodynamic radii were measured with a DynaPro-801 TC dynamic light scattering instrument with a MicroCell attachment and Dynamics 3.3 software (Protein Solutions Inc., Charlottesville, VA). The instrument calibration was checked with a 2 mg/ml aqueous solution of bovine serum albumin. We measured hydrodynamic radii of soluble particles in the organic phases after solubilization with 20% TFIP + 1% AOT and 20% isooctane + 2% AOT with and without protein. Refractive indices and densities for TFIP and isooctane were used as published (Timmermans, 1950). Samples were filtered with centrifuge filters with a 0.2 μm nylon membrane (Osmonics, Livermore, CA) before dynamic light scattering measurements.

Proteinase K digestion assays

Vials containing PrP 27-30 solubilization samples were left open overnight at RT to remove organic solvents that have been found to inactivate PK (Wille et al., 1996). After evaporation of the solvents, the samples were resuspended to the original volume by addition of water, and PrP 27-30 concentrations were kept at the levels achieved by solubilization (Figs. 1 and 5). PK was added to a concentration of 87.5 μg/ml. The reaction mix was incubated at 37°C for 2 h. The reaction was stopped by adding 5 mM PMSF and one-half volume of SDS sample buffer. All samples were boiled for 5 min at 100°C before gel electrophoresis.

FTIR

FTIR analysis of PrP 27-30 after solubilization was carried out on samples with up to 1 mg/ml protein in D_2O-containing buffers. Solubilization assays were performed as in previous experiments except for the use of D_2O instead of H_2O. FTIR spectra were recorded with a Perkin-Elmer (Norwalk, CT) System 2000 FTIR spectrophotometer with a microscope attachment. The sample was enclosed between 2 AgCl windows (International Crystal Laboratories, Garfield, NJ), creating a pathlength of 50 μm within an airtight sealed chamber. Spectra were recorded in the amide 1′ region between 1750 cm^{-1} and 1550 cm^{-1}. Blank controls identical in the concentrations of detergents and solvents were used to subtract any nonprotein contributions from the spectra. Spectral analysis and self-deconvolution were carried out as previously described (Byler and Susi, 1986) and modified (Gasset et al., 1993).

Sucrose gradient ultracentrifugation

The gradients were produced using a Beckman SW 60Ti rotor at 60,000 rpm and 20°C. The centrifugation was set to reach an $\int\omega^2 dt$ of $1.25 \cdot 10^{12}$ rad^2/s; the value was chosen to pellet particles with a density of ~1.3 g/ml and an $S_{20,w}$ value of 8 S and above. Linear gradients contained 5–20% sucrose with 10 mM NaHEPES, 50 μM NaN_3 pH 7.4 with or without 1% TFIP, and 0.5% AOT. The gradient volume was 4 ml with a 400-μl sample carefully layered onto the top of the sucrose gradient. PrP 27-30 samples were solubilized by 20% TFIP + 1% AOT. The high density of TFIP made it necessary to dilute the PrP 27-30 sample by a factor of 4 with 10 mM NaHEPES, 50 μM NaN_3, pH 7.4. This dilution step reduced the PrP 27-30 concentration and the scrapie titer considerably but was necessary to prevent the mixing of the sucrose gradient with the sample before centrifugation. After the centrifugation run, the gradients were harvested from the top into ~250-μl aliquots. The sedimentation coefficients were calculated (Steensgaard et al., 1978). The specific volume for PrP 27-30 was calculated (Durchschlag, 1986), assuming that PrP 27-30 contained 77% protein (~16,240 Da; aa 90–231) with a specific volume of 0.71 cm^3/g; 14% lipid [~2975D in the GPI anchor (Stahl et al., 1992)] with a specific volume of 1 cm^3/g and 9% polysaccharide [~1955 Da (Endo et al., 1989)] with a specific volume of 0.61 cm^3/g. Taken together, PrP 27-30 should have a specific volume of ~0.74 cm^3/g (or a density of ~1.35 g/ml). The influence of potentially bound AOT molecules on the density of PrP 27-30 was not taken into account in this estimation. We performed an independent calculation of sedimentation coefficients that employs standard proteins with known $S_{20,w}$ values such as ribonuclease A with 1.6 S and ovalbumin with 3.6 S (Steensgaard et al., 1992) and compares the distances ribonuclease A, ovalbumin, and PrP 27-30 migrated in the sucrose gradient.

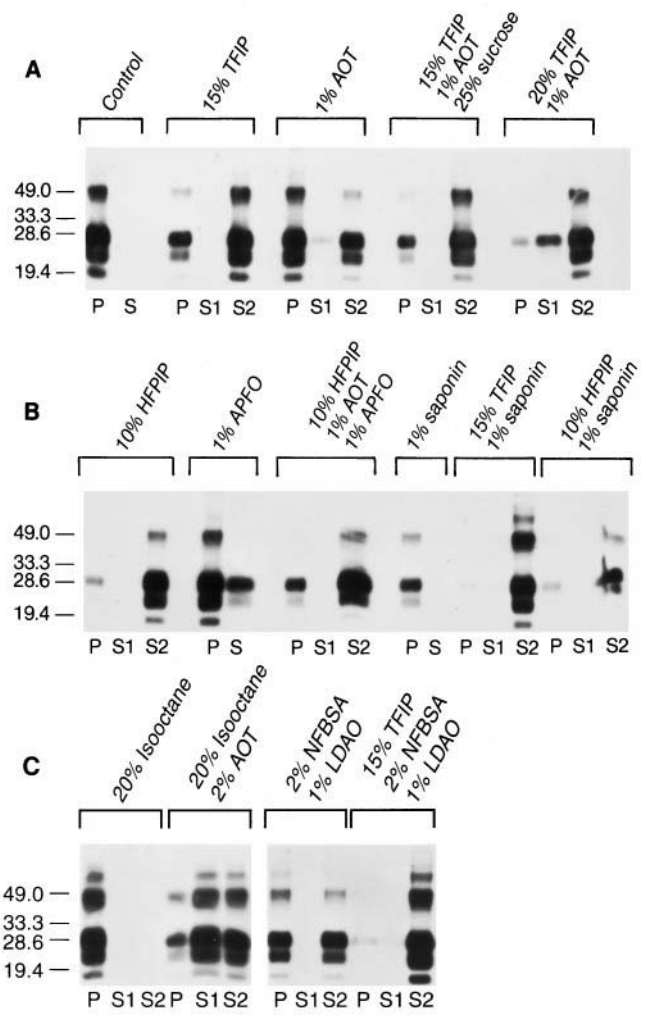

FIGURE 1 Western blots of PrP 27-30 after solubilization by organic solvents, detergents, or combinations. Samples were centrifuged at 100,000 × *g* for 1 h and then separated into pellet and supernatant fractions. The supernatants were split into organic and aqueous phases wherever applicable, with the top phase labeled S1 and the bottom phase labeled S2. The S2 phases of solubilization samples 1% AOT and 2% NFBSA in 1% LDAO showed considerable viscosity, warranting the term detergent pellet more than supernatant 2. The control (buffer only) showed all PrP 27-30 in the pellet. Some organic solvents alone, such as TFIP and HFPIP, showed considerable solubilization, while detergents alone (AOT, APFO, and saponin) resulted in less solubilization. Combinations of solvents and detergents gave the best results as judged by ultracentrifugation.

RESULTS

Solubilization assays

In an earlier study, we reported that α-helix-promoting solvents such as HFIP or TFIP disrupt polymers of PrP 27-30 (prion rods) into smaller, more regular structures

(Wille et al., 1996). This partial disaggregation seems to have been caused by the conversion of intermolecular antiparallel β-sheets into α-helical structures, a process that could be visualized by a reduction in Congo red dye binding corresponding to the decrease of amyloid character. In the investigations reported here, we set out to use these properties to solubilize the highly aggregated PrP 27-30, thereby making it practical to attempt crystallization as well as other biophysical and biochemical methods.

Of a large number of solvents and detergents tested, only a few yielded any solubilization of PrP 27-30 as judged by ultracentrifugation at 100,000 $\times$ *g* for 1 h (Table 1). The most promising conditions using solvents or detergents alone were then combined to test whether any of those were sufficient to overcome the β-sheet and hydrophobic interactions observed in these aggregates. Fig. 1 *A* shows that untreated PrP 27-30 (control) was pelleted owing to its aggregated nature. Organic solvents and detergents alone led at best to a limited amount of PrP 27-30 in the supernatants, and only combinations of some solvents and detergents resulted in a virtually complete solubilization (Fig. 1, *A–C*). Early on we observed that the best results were achieved with conditions that caused a separation into two liquid phases, either during the incubation at 37°C or later at the 100,000 $\times$ *g* ultracentrifugation. Consistently, PrP 27-30 was found primarily in the organic phase and at the interphase. The organic phase was at the bottom of the tube for TFIP and HFPIP because of the high density of the fluorinated alcohol, while the low-density isooctane caused the organic phase to float above the aqueous buffer. Repeatedly, we observed that insoluble protein did not pellet, but remained trapped at the interphase because of the high density of the organic phase. We avoided contamination of the organic phase for further experiments by carefully separating the phases after ultracentrifugation. We found that negative stain electron microscopy of the supernatants was useful in determining whether solubilization had occurred or aggregates of PrP 27-30 were floating.

Solubilization of a protein or hydrophilic molecule into a hydrophobic organic solvent is usually achieved through reverse micelles. Because the detergent AOT is frequently used in studies of reverse micelles, we tested whether solubilization occurred via this mechanism as well. Contrary to solubilization in aqueous systems, the solubilization in reverse micelles through AOT is favored at about one pH unit below the IEP of the protein and decreases at pH values further away from the IEP (Göklen and Hatton, 1987; Wolbert et al., 1989). Subsequently we found that PrP 27-30 is preferentially solubilized at pH ~8.0 (with its IEP near pH 9.0) with a decrease in solubilization at lower pH and at pH values around and above the IEP of PrP 27-30 (data not shown). Therefore, it appears that PrP 27-30 is solubilized by reverse micelles formed by the detergent AOT in the solvents TFIP, HFPIP, or isooctane, respectively. The solubilization through isooctane + AOT was less reproducible than the other conditions tested. We investigated the cause of these problems and observed that hydrolysis products of aged AOT solutions had a pronounced negative effect on

TABLE 1 Effects of some solvents, detergents, and combinations used for solubilization of PrP 27-30

Solubilizing agent	% Solubilized (100,000 $\times$ *g* supernatant)	Electron microscopy of supernatant
TFIP (5–20%)	up to ~75%	small aggregates
HFIP (1.25–25%)	up to ~20%	small aggregates
HFPIP (1.25–10%)	up to ~75%	rod fragments
Dimethylsulfoxide (5–20%)	<5%	n.d.*
AOT (0.25–2%)	up to ~50%	rods and rod fragments
Saponin (0.25–1%)	up to ~10%	rods and rod fragments
APFO (0.5–5%)	up to ~30%	amorphous aggregates
LDAO (0.25–1%)	up to ~5%	n.d.
Digitonin (0.25–1%)	0	n.d.
2.5% NFBSA in 1% AOT	up to ~10%	rods and rod fragments
2% NFBSA in 1% LDAO	up to ~50%	no aggregates detectable
15–20% TFIP + 1% AOT	up to ~75%	no aggregates detectable
15% TFIP + 1% AOT + 25% sucrose	>90%	no aggregates detectable
15% TFIP + 1% AOT + 1% APFO	<10%	n.d.
15% TFIP + 1% AOT + 2.5% NFBSA	~10%	n.d.
15% TFIP + 1% LDAO + 2% NFBSA	>90%	no aggregates detectable
15% TFIP + 1% saponin	>90%	no aggregates detectable
10% HFPIP + 1% AOT	~10%	n.d.
10% HFPIP + 1% AOT + 25% sucrose	~10%	rod fragments
10% HFPIP + 1% AOT + 1% APFO	>90%	no aggregates detectable
10% HFPIP + 1% AOT + 2.5% NFBSA	viscous phase#	n.d.
10% HFPIP + 1% LDAO + 2% NFBSA	>90%	some rod fragments
10% HFPIP + 1% saponin	>90%	saponin micelles only
10% HFPIP + 2% APFO	>90%	rod fragments
20% Isooctane + 2% AOT	up to ~80%	no aggregates detectable

*n.d., not determined.

#The increased viscosity prevents proper separation.

solubilization via isooctane + AOT and much less so on the other combinations. The hydrolysis product 2-ethylhexanol effectively abolished the solubilizing action of isooctane + AOT, while another major hydrolysis product, sulfosuccinic acid, had a beneficial effect (data not shown). The detergents saponin or NFBSA/LDAO are not usually known to form reverse micelles, but we think this solubilization mechanism could apply here as well.

Negative staining allowed us to check the aggregation state of solubilized proteins found in the supernatant fractions. Organic solvents such as TFIP or HFPIP alone reduced the aggregate size, but did not fully solubilize PrP 27-30 (Fig. 2, *B* and *C*). Detergents alone influenced the structure of PrP 27-30 aggregates even less, barely changing rod shape and ultrastructure (Fig. 2, *D–F*). Only combinations of solvents and detergents led to a complete disappearance of rod-shaped aggregates (Fig. 2, *A* and *G–J*). The "doughnut"-shaped structures in Fig. 2 *J* are saponin micelles that have been described elsewhere (Bomford et al., 1992; Kersten et al., 1991). Electron microscopy revealed that solubilization occurred only in conditions when α-helix-promoting solvents and detergents were used together. The widely used solubilization criterion of a 1-h ultracentrifugation at 100,000 $\times$ *g* was clearly insufficient to judge solubilization of PrP 27-30 (compare Riesner et al., 1996).

Dynamic light scattering of solubilized PrP

The use of dynamic light scattering allowed us to confirm our notion that PrP 27-30 is solubilized into reverse mi-

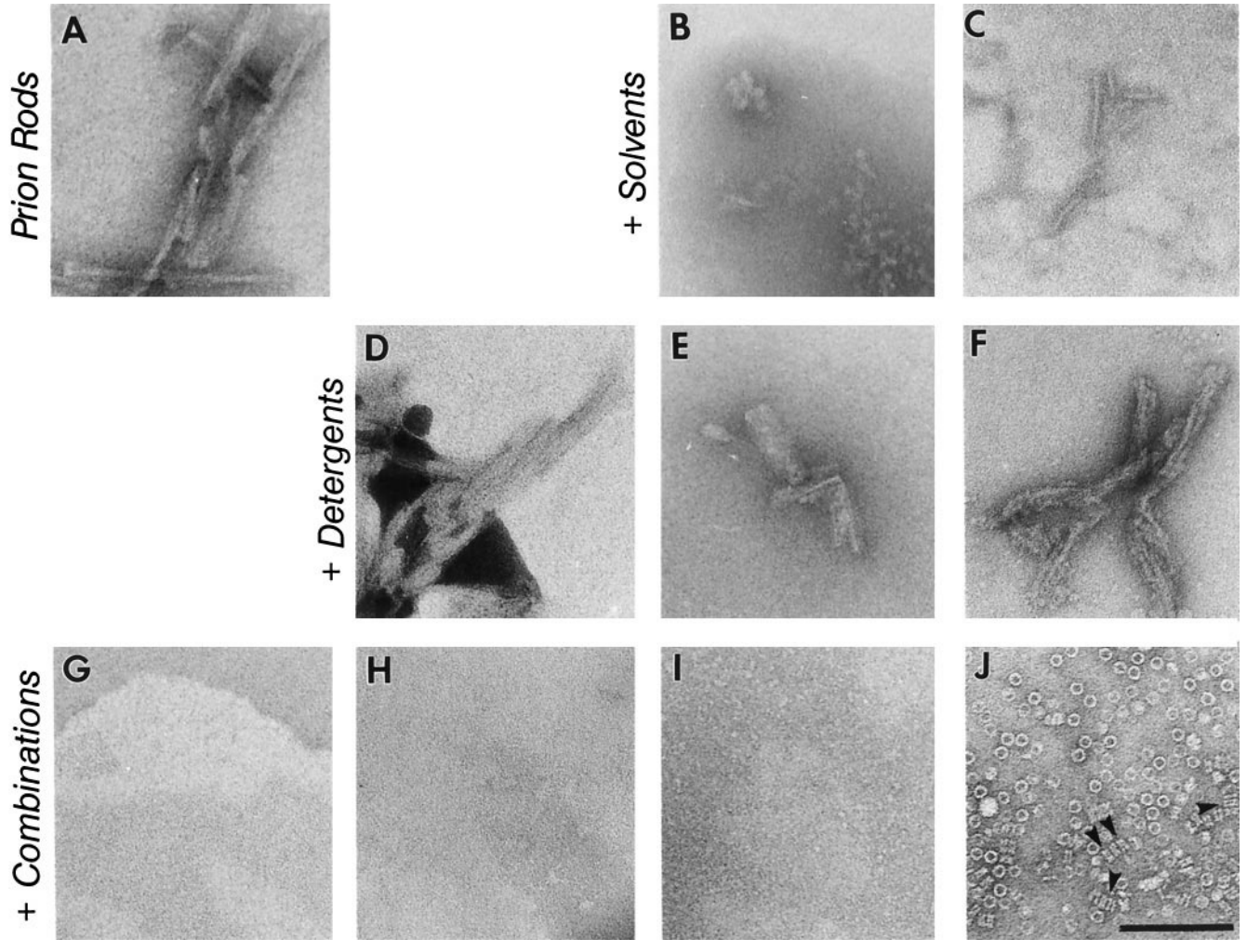

FIGURE 2 Negative stain electron microscopy of PrP 27-30 before and after solubilization. (*A*) Highly aggregated prion rods. (*B*) Organic phase (supernatant 2) of PrP 27-30 "solubilized" by 15% TFIP showing amorphous aggregates of various sizes. (*C*) PrP 27-30 treated with 10% HFPIP (supernatant 2) yields small linear polymers. (*D*) Treatment with 1% AOT changed the rod structure but did not disaggregate PrP 27-30 polymers. 1% APFO (*E*) or 1% saponin (*F*) had little effect on rod structure. The electron micrographs (*B–F*) show that in all cases, neither solvents nor detergents alone truly solubilized PrP 27-30, but only prevented the aggregates from pelleting during ultracentrifugation. (*G*) The combination of 15% TFIP + 1% AOT + 12.5% sucrose truly solubilized PrP 27-30, as no protein aggregates could be detected by negative stain electron microscopy (supernatant 2). (*H*) Supernatant 2 after treatment with a combination of 10% HFPIP + 1% AOT + 1% APFO was void of protein aggregates as well. Even the combinations of 15% TFIP + 1% saponin (*I*) and 10% HFPIP + 1% saponin (*J*) showed no apparent protein aggregates. The latter combination showed small doughnut-shaped saponin micelles, which can be seen in the top view and occasionally (*arrowheads*) from the side. Negative stain 2% ammonium molybdate. Bar = 100 nm.

celles. Solubilization controls consisting of TFIP + AOT without protein showed two peaks with a very narrow distribution: water-filled reverse micelles with a hydrodynamic radius of ~5.3 nm and detergent aggregates with a hydrodynamic radius of ~0.9 nm. Upon solubilization of PrP 27-30, the pool of reverse micelles became polydispersed and disproportionated into smaller water-filled reverse micelles and larger reverse micelles that contain protein (data not shown). A similar behavior has been described for the uptake of proteins into AOT + isooctane reverse micelles (Zampieri et al., 1986). PrP 27-30 solubilized into isooctane + AOT revealed the presence of unexpectedly large reverse micelles with a hydrodynamic radius of ~46 nm (data not shown). Blank control samples under identical conditions could not be measured with dynamic light scattering because of the presence of very large particles (presumably detergent aggregates) that interfered with measurements.

Crystallization of solubilized PrP

While examining negatively stained preparations of solubilized PrP 27-30 by electron microscopy, we found that under some conditions, PrP crystallized into microscopic two- and three-dimensional crystals (Fig. 3). Formation of these crystals was found to require uranyl salts containing acetate, formate, or nitrate. Other metal salts used for negative staining such as ammonium molybdate, sodium phosphotungstate, copper sulfate, zinc sulfate, bismuth oxynitrate, bismuth nitrate, thallium acetate, lead acetate, cadmium iodide, lanthanum nitrate, vanadylsulfate, and aurothioglucose did not promote the formation of PrP crystals. Blank controls that lacked PrP 27-30, but were otherwise treated identically, did not show any crystalline arrays, but revealed micelles of various shapes and large detergent aggregates (data not shown).

In our characterization of the conditions for crystal growth we found that an acidic pH of 4.0 or lower was essential. A pH close to 4.0 promoted the growth of two-dimensional crystals (Fig. 3 *B*), while pH values at 3.5 or lower increased the number and size of three-dimensional crystals (Fig. 3 *A*). We used 50 mM sodium acetate as a buffer and found that 50 mM sodium citrate did not support the growth of PrP 27-30 crystals. During the process of negative staining it was essential for the reproducible growth of crystals that some detergent be removed by washing with uranyl solution. However, excess washing destroyed all crystals that formed intermittently; this suggests that some amount of detergent is probably required to maintain crystalline order. Interestingly, we infrequently observed almost identical protein crystals grown from PrP 27-30 in 15% TFIP + 1% LDAO + 2.5% NFBSA, which shows that the detergent AOT was not essential for crystal growth (data not shown).

PrP 27-30 solubilized by different combinations of detergents and solvents produced several types of crystals (Fig. 3, *A* and *B* versus *E* and *F*). Lattice spacings were determined from electron micrographs and by electron diffraction (compare Table 2 and Fig. 4). The three-dimensional crystals obtained from TFIP + AOT seemed to be seeded by underlying two-dimensional arrays, as could be seen by tilted specimens (Fig. 3, *C* and *D*). PrP 27-30 solubilized by HFPIP + AOT + APFO resulted in arrays with a distinct crystal lattice (Fig. 3 *E* and Table 2). Crystals grown from PrP 27-30 in isooctane + AOT show a high contrast, which indicates multiple layers and a pronounced tendency to grow in three dimensions (Fig. 3 *F* and Fig. 4). In this preparation, at least four different types of crystals could be observed; it is conceivable that these represent views from different directions.

Prion infectivity and PK resistance of solubilized PrP

Bioassays of PrP 27-30 from solubilization experiments showed that substantial amounts of infectivity could be found in the supernatant fractions after treatment with organic solvents or detergents alone. Solubilization by combinations of TFIP + AOT + sucrose or TFIP + saponin led to a titer in the organic phase (S2) that was 10–1000 times higher than that of the pellet fraction (Table 3). Other combinations that showed good solubilization, such as TFIP + LDAO + NFBSA or isooctane + AOT, carried approximately equal amounts of infectivity in the supernatant and pellet fractions. Experiments using the solvent HFPIP either in combination with detergent or alone (Fig. 1 *B*) invariably abolished scrapie infectivity.

Treatment with organic solvents and detergents not only changed the aggregation state of PrP 27-30, but it also modified its resistance to PK digestion (Fig. 5). The control pellet and PrP 27-30 treated by TFIP alone remained resistant to PK digestion. Supernatant fractions containing PrP 27-30 treated with HFPIP, APFO, or a combination of both lost all resistance to PK digestion, while PrP 27-30 treated with AOT and combinations of AOT and TFIP showed a substantial reduction in resistance to PK digestion (Fig. 5).

Although disaggregation of PrP 27-30 was generally accompanied by a diminution in the resistance of the protein to digestion by PK, the exceptions to this rule are most important. Even partial disaggregation, as seen with HFPIP or APFO (see Fig. 2), led to a reduction in PK resistance. However, treatment with TFIP disrupted PrP 27-30 aggregates without reducing PK resistance, showing that the aggregation state does not always correlate with PK resistance (Figs. 2 and 5). Bioassays showed that prion rods treated with APFO retained full infectivity, while samples treated with HFPIP or a combination of APFO and HFPIP lost infectivity (Table 3). That these three conditions abolish PK resistance equally well (Fig. 5) but have different effects on scrapie infectivity demonstrates that PK resistance is not required for preservation of prion infectivity. This finding is in accord with other studies on transgenic mice expressing

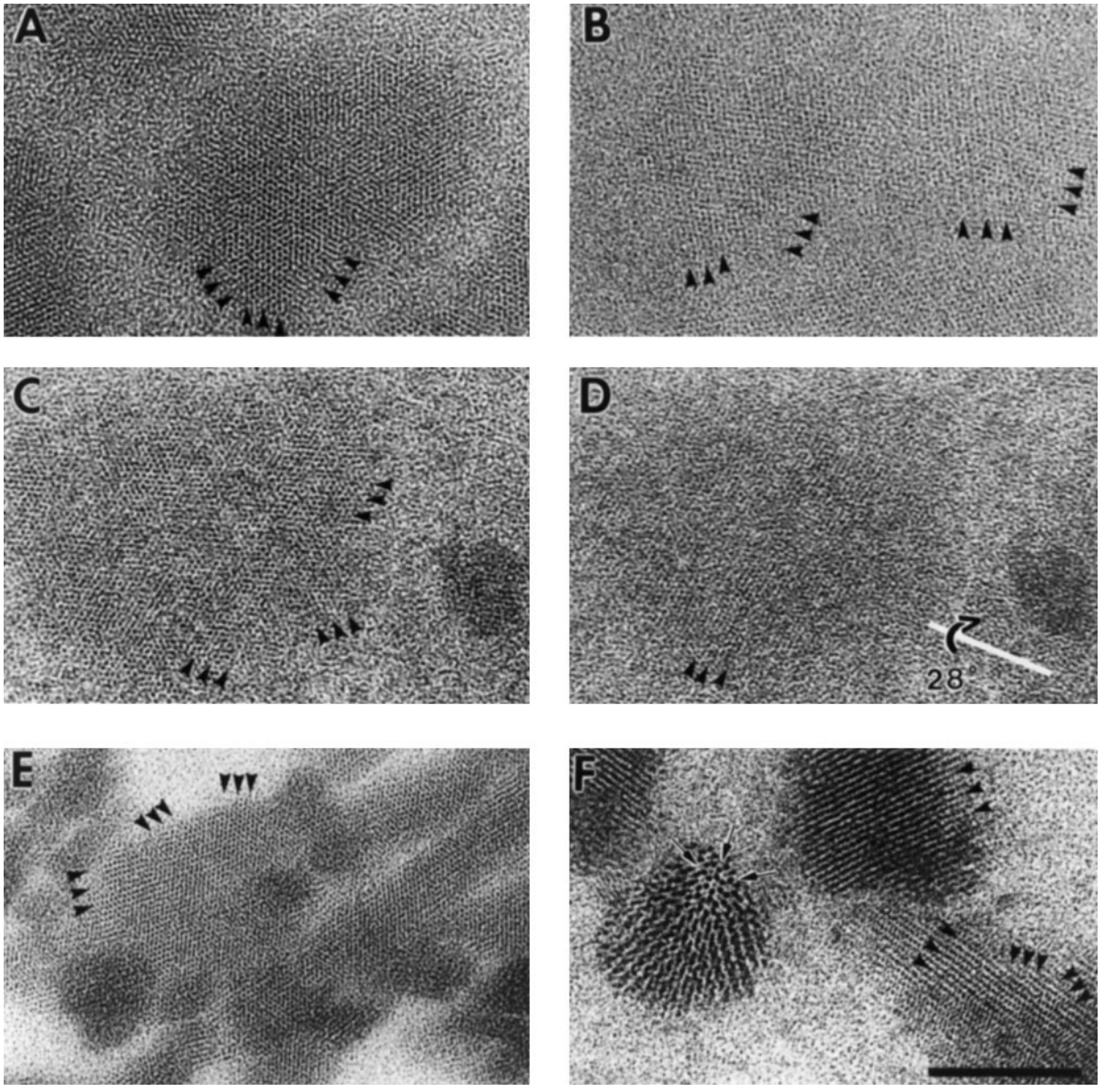

FIGURE 3 Electron microscopy on two- and three-dimensional crystals of PrP 27-30. (*A*) Small three-dimensional crystals of PrP 27-30 solubilized by 20% TFIP + 1% AOT with a hexagonal pattern. (*B*) Two-dimensional crystals of PrP 27-30 solubilized by 20% TFIP + 1% AOT. (*C*) Untilted electron micrograph of a small three-dimensional crystal similar to (*A*). (*D*) Same crystal as in (*C*) but tilted by 28°. A two-dimensional crystal lattice could be seen after tilting, indicating that two-dimensional crystals seem to seed the three-dimensional ones. (*E*) Two- and three-dimensional crystals of PrP 27-30 solubilized by 10% HFPIP + 1% AOT + 1% APFO. These crystals were grown by using unbuffered 2% uranyl acetate solution. (*F*) Two- and three-dimensional crystals of PrP 27-30 solubilized by 20% isooctane + 2% AOT grown with buffered uranyl acetate pH 4.0. Three different lattices can be observed. Bar = 100 nm.

the P101L mutation that generates infectivity spontaneously (Hsiao et al., 1994; Telling et al., 1996a) and on a PK-sensitive fraction of PrP^{Sc} that correlates with the length of the incubation period (Safar et al., 1998).

Sedimentation coefficients of solubilized PrP

We performed sucrose gradient centrifugation to determine the molecular size and aggregation state of solubilized PrP 27-30. The high density of TFIP made it necessary to dilute PrP 27-30 samples with aqueous buffer. This step led, most likely, to a reextraction of the protein into the aqueous phase since no phase separation was present after dilution. A standard gradient with 5–20% sucrose without addition of either detergent or solvent led to a complete reaggregation during centrifugation (data not shown). The addition of 1% TFIP and 0.5% AOT to the gradient allowed PrP 27-30 to remain soluble and to migrate according to its size, shape, and density (Fig. 6 *A*). Calculation of the $S_{20,w}$ values revealed that the majority of solubilized PrP 27-30 migrated as monomers of ~2 S, and a small fraction of the protein migrated around 4 S, which corresponds to PrP 27-30

TABLE 2 Electron diffraction data on PrP 27-30 crystals prepared with uranyl salts

Solubilization fraction		Crystals	Electron diffraction results
15% TFIP 1% AOT	supernatant 2	2D crystals 3D crystals	4.0–3.9 nm on both axes, 68°–70° angle 3.7 nm, hexagonal array higher-order reflections at 2.2 nm and 1.85 nm
15% TFIP 1% AOT 25% sucrose	supernatant 2	Same as above	
10% HFPIP 1% AOT 1% APFO	supernatant 2	2D/3D crystals	3.5 nm and 3.0 nm, 68° angle
5% HFPIP 1% AOT 25% Sucrose	supernatant 2	Crystals too small for electron diffraction	
15% TFIP 1% LDAO 2.5% NFBSA	supernatant 2	Crystals too small for electron diffraction	
20% Isooctane 2% AOT	supernatant 1	3D crystals type I type II type III	 5.0 nm and 3.1 nm, 71°/109° angle, Fig. 4 *A* 8.7 nm, 4.35 nm, and 5.1 nm, 29° angle, Fig. 4 *B* ~9.1 nm, hexagonal array higher-order reflections at ~5.0 nm, Fig. 4 *C*

dimers. The pelleted PrP 27-30 had a sedimentation coefficient of >8 S. An independent confirmation of the $S_{20,w}$ values calculated from the first set of sucrose gradients was obtained by use of standard proteins such as ribonuclease A and ovalbumin. $S_{20,w}$ values calculated from these gradients (Fig. 6 *B*) matched those calculated without the use of calibrated proteins (Fig. 6 *A*); thus, we were able to calculate the sedimentation coefficients by two independent methods.

Bioassays of fractions from three independent sucrose gradients revealed that prion infectivity could be found only in the pellet fractions (Fig. 6 *C*). All scrapie prion infectivity that was loaded onto the gradients, as determined by separate bioassays, was recovered in the pellets, showing that only 10% of PrP 27-30 accounted for all infectious units while the remaining 90% could be separated from infectivity (Fig. 6). Ultracentrifugation without solvent or detergent in the gradient (see above) led to reaggregation and pelleting of PrP 27-30, and all of the infectivity that remained after solubilization was found in the pellet as well. Negative staining did not show protein aggregates in the peak fractions of monomeric and dimeric PrP (Fig. 6, *D* and *E*). The pellet fraction contained a small number of PrP aggregates showing morphological features of prion rods (Fig. 6 *F*) indicating the PrP 27-30 had not been solubilized.

FTIR spectroscopy

Previously, we observed that PrP 27-30 sustained a sizable reduction in β-sheet structure upon exposure to α-helix-promoting solvents such as HFIP or TFIP (Wille et al., 1996). Those studies were carried out in the presence of high concentrations of sucrose because of experimental constraints. Here, to our surprise, we found that the β-sheet content remained almost constant throughout treatments with either detergents or solvents (Table 4). Only a combination of detergent and solvent with sucrose (15% TFIP + 1% AOT + 12.5% sucrose) showed a significant decrease in β-sheet structure. This shift from β-sheet to α-helix was similar to the change observed in our earlier study indicating that sucrose is an essential component for this conformational transition. PrP 27-30 solubilized by HFPIP + AOT + APFO could not be analyzed by FTIR spectroscopy because of uninterpretable variations in absorption patterns (data not shown).

DISCUSSION

Although the insolubility of prion infectivity in nondenaturing detergents has been a persistent problem (Millson et al., 1976; Prusiner et al., 1978), it was used to enrich fractions from Syrian hamster brain that led to the discovery of PrP 27-30 (Bolton et al., 1982; Prusiner et al., 1982). The hydrophobic nature of prions and their close association with membranes complicated efforts to obtain purified preparations (Kimberlin et al., 1971; Malone et al., 1978; Marsh et al., 1984; Millson et al., 1971; Semancik et al., 1976). Even after PrP^{Sc} was discovered, it proved difficult to release PrP^{Sc} from its association with membranes (Safar et al., 1991).

Dispersion of PrP 27-30 into DLPCs increased the prion titer by as much as 10-fold (Gabizon et al., 1987, 1988), but the lipids interfered with crystallization and many biophysical methods of analysis, rendering this procedure impractical. Intermediate concentrations of GdnHCl (1.5–4.5 M) allowed a moderate level of solubilization (Safar et al., 1993) but again did not permit crystallographic studies. More recently, use of ~0.2% SDS and sonication led to

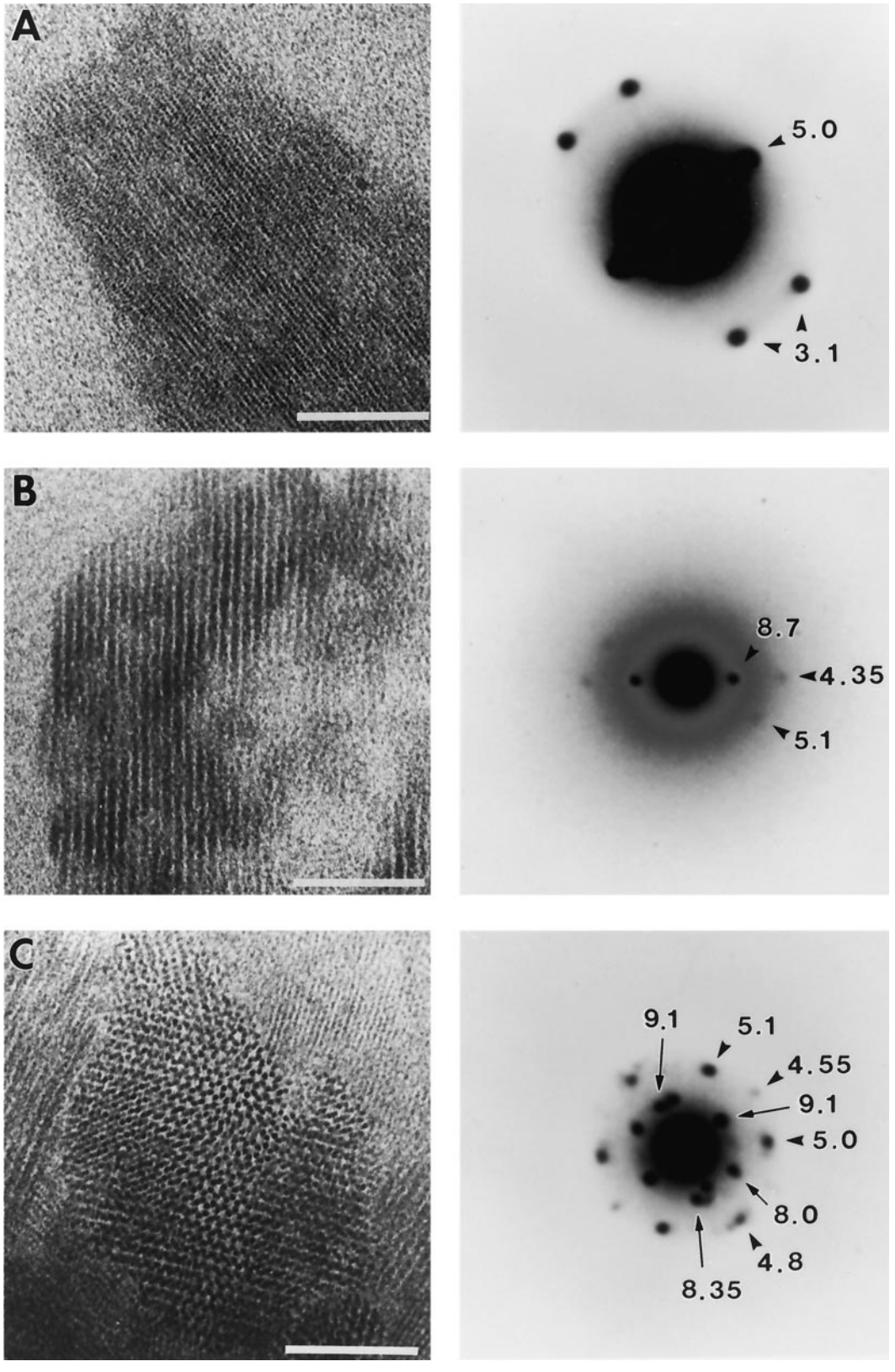

FIGURE 4 Electron micrographs and electron diffractograms of PrP 27-30 crystals. PrP 27-30 was solubilized by 20% isooctane + 2% AOT, crystals were grown from supernatant 1 by use of buffered uranyl acetate pH 4.0. Crystals with three different lattices were analyzed by electron diffraction. The distances of the diffraction spots are given in nanometers. Bar = 100 nm.

TABLE 3 Scrapie infectivity of PrP 27-30 after solubilization

Assay conditions		Titer log ID_{50}/ml (n/n_0)*									
		Experiment 1		Experiment 2		Experiment 3		Experiment 4		Experiment 5	
PrP 27-30, untreated control		7.5	(4/4)	8.2	(4/4)	8.8	(4/4)	9.3	(4/4)	8.7	(4/4)
PrP 27-30 buffer control	pellet	6.7	(4/4)	8.3	(4/4)	9.4	(4/4)	9.3	(4/4)	8.7	(4/4)
	supernatant	1.8	(1/4)	3.8	(4/4)	3.2	(3/4)	3.7	(4/4)	4.6	(4/4)
PrP 27-30 + 15% TFIP	pellet	6.4	(4/4)	n.d.[#]		7.5	(4/4)	8.4	(4/4)	n.d.	
	supernatant 1	n.d.		n.d.		4.3	(4/4)	2.7	(3/4)	n.d.	
	supernatant 2	3.3	(2/4)	n.d.		7.8	(4/4)	7.1	(4/4)	n.d.	
PrP 27-30 + 1% AOT	pellet	6.7	(4/4)	n.d.		9.1	(4/4)	9.3	(4/4)	n.d.	
	supernatant 1	n.d.		n.d.		5.7	(4/4)	7.2	(4/4)	n.d.	
	supernatant 2	7.8	(4/4)	n.d.		9.4	(4/4)	9.3	(4/4)	n.d.	
PrP 27-30 + 15% TFIP	pellet	3.1	(2/4)	5.2	(4/4)	6.2	(4/4)	6.2	(4/4)	n.d.	
+ 1% AOT	supernatant 1	n.d.		2.5	(4/4)	2.6	(4/4)	3.3	(4/4)	n.d.	
+ 25% sucrose	supernatant 2	6.2	(4/4)	8.2	(4/4)	7.2	(4/4)	7.2	(4/4)	n.d.	
PrP 27-30 + 10% HFPIP	pellet	<1	(0/4)	n.d.		1.3	(1/4)	<1	(0/4)	n.d.	
	supernatant 1	n.d.		n.d.		<1	(0/4)	1.7	(2/4)	n.d.	
	supernatant 2	<1	(0/4)	n.d.		3.7	(4/4)	7.4	(3/4)	n.d.	
PrP 27-30 + 1% APFO	pellet	n.d.		n.d.		9.0	(4/4)	10.0	(4/4)	n.d.	
	supernatant	n.d.		n.d.		8.0	(4/4)	7.1	(4/4)	n.d.	
PrP 27-30 + 10% HFPIP	pellet	n.d.		<1	(0/4)	<1	(0/4)	<1	(0/4)	n.d.	
+ 1% AOT	supernatant 1	n.d.		<1	(0/4)	<1	(0/4)	<1	(0/4)	n.d.	
+ 1% APFO	supernatant 2	n.d.		<1	(0/4)	<1	(0/4)	<1	(0/4)	n.d.	
PrP 27-30 + 15% TFIP	pellet	3.1	(3/4)	5.8	(4/4)	n.d.		n.d.		n.d.	
+ 1% saponin	supernatant 1	n.d.		n.d.		n.d.		n.d.		n.d.	
	supernatant 2	6.7	(4/4)	6.9	(4/4)	n.d.		n.d.		n.d.	
PrP 27-30 + 10% HFPIP	pellet	<1	(0/4)	2.7	(4/4)	n.d.		n.d.		n.d.	
+ 1% saponin	supernatant 1	n.d.		<1	(0/4)	n.d.		n.d.		n.d.	
	supernatant 2	<1	(0/4)	<1	(0/4)	n.d.		n.d.		n.d.	
PrP 27-30 + 1% LDAO	pellet	n.d.		7.4	(4/4)	n.d.		n.d.		n.d.	
+ 2% NFBSA	supernatant	n.d.		7.4	(4/4)	n.d.		n.d.		n.d.	
PrP 27-30 + 15% TFIP	pellet	n.d.		6.6	(4/4)	n.d.		n.d.		n.d.	
+ 1% LDAO	supernatant 1	n.d.		n.d.		n.d.		n.d.		n.d.	
+ 2% NFBSA	supernatant 2	n.d.		7.3	(4/4)	n.d.		n.d.		n.d.	
PrP 27-30 + 20% isooctane	pellet	n.d.		n.d.		n.d.		n.d.		8.0	(4/4)
	supernatant 1	n.d.		n.d.		n.d.		n.d.		4.6	(4/4)
	supernatant 2	n.d.		n.d.		n.d.		n.d.		4.9	(4/4)
PrP 27-30 + 20% isooctane	pellet	n.d.		n.d.		n.d.		n.d.		7.3	(4/4)
+ 2% AOT	supernatant 1	n.d.		n.d.		n.d.		n.d.		7.4	(4/4)
	supernatant 2	n.d.		n.d.		n.d.		n.d.		7.4	(4/4)

*n/n_0, number of sick animals/number of inoculated animals.
[#]n.d., not determined.

disaggregation of PrP 27-30 into small spherical particles with a relatively homogeneous size distribution of ~10 nm and a $S_{20,w}$ value of ~6 S (Riesner et al., 1996), but this procedure failed to produce monomers or dimers of PrP 27-30.

From previous investigations using α-helix-promoting solvents, we surmised that these solvents might have the potential to disaggregate prion rods (Wille et al., 1996). In the study reported here, we learned that neither organic solvents nor nondenaturing detergents alone were sufficient to solubilize PrP 27-30 (Fig. 1 and Table 1). Although many membrane proteins can be solubilized by mild non-ionic detergents, they have been found to lose activity when stronger ionic detergents are used. In the case of prions, the polymers of PrP 27-30 were found to withstand even the most potent ionic detergents. Only combinations of one or more detergents and organic solvents showed substantial solubilization of PrP 27-30 (Fig. 1 and Table 1).

Solubilization of PrP via reverse micelles

Although solubilization is generally monitored by ultracentrifugation at 100,000 × *g* for 1 h, this proved to be inadequate for monitoring solubilization of PrP 27-30 (Riesner et al., 1996). In many cases, negative stain electron microscopy revealed the presence of protein aggregates in supernatant fractions (Fig. 2), so we regularly performed negative staining on 100,000 × *g* supernatant fractions. Since solubilization with a high yield was achieved only when a phase separation into two liquid phases occurred, we suspected a solubilization mechanism involving reverse micelles. The pH dependency of solubilization by reverse micelles that had been observed for proteins such as ribonuclease A, cytochrome C, and elastase (Göklen and Hatton, 1987; Wolbert et al., 1989) suggested an approach to optimize the solubilization further by increasing the pH to a value just below the IEP of PrP 27-30. A conventional

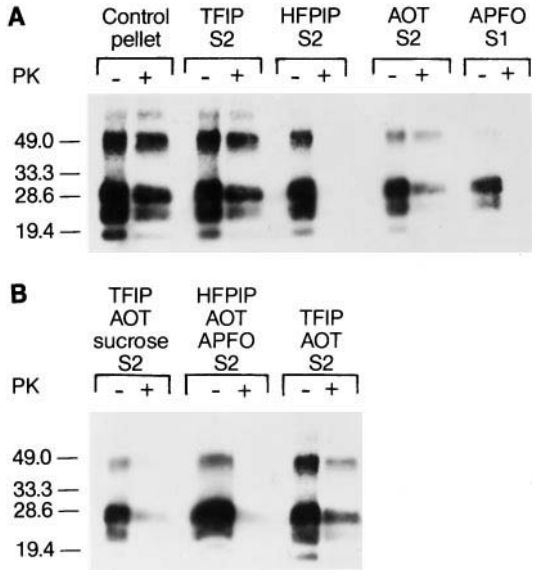

FIGURE 5 Western blots of PK assays on PrP 27-30 after solubilization. The supernatants after solubilization by various agents were incubated with PK for 2 h at 37°C. Solubilization by 10% HFPIP, 1% APFO, 10% HFPIP + 1% AOT + 1% APFO, or 15% TFIP + 1% AOT + 12.5% sucrose almost completely abolished PK resistance in PrP 27-30. Treatment by 1% AOT or 20% TFIP + 1% AOT reduced PK resistance, while 15% TFIP alone had no significant effect.

solubilization mechanism would require a pH distinctly different from the IEP. The limited solubilization that was achieved using 2.5% NFBSA in 1% LDAO showed this type of pH dependency, implying that a conventional mechanism of solubilization might be occurring with this combination (data not shown).

The solubilization capacity of AOT reverse micelles is influenced by cosolvents and cosurfactants, which can include autohydrolysis products (Fletcher et al., 1982; Rabie et al., 1997). One AOT hydrolysis product, 2-ethylhexanol, reduces the solubilization yield in the system isooctane + AOT but not with TFIP + AOT. Substoichiometric amounts of 2-ethylhexanol improve the solubility of AOT monomers in apolar solvents, such as isooctane, and thereby effectively reduce the concentration of solubilization-competent reverse micelles. Another AOT hydrolysis product, sulfosuccinic acid, increases solubilization in isooctane + AOT by salting AOT out of the aqueous phase and into the organic phase, and hence elevates the concentration of reverse micelles (Fletcher et al., 1982; Rabie et al., 1997). TFIP as an alcohol behaves differently from the usually employed solvents and thereby makes this solubilization system much less vulnerable to chemical impurities and physical disturbances.

In summary, we think PrP 27-30 was solubilized into reverse micelles based on the following observations: 1) the majority of PrP 27-30 could be found in the organic phase only (Fig. 1); 2) conditions that did not separate into an aqueous and organic phase yielded little or no solubilization (Table 1); 3) the solubilization showed an optimum at about one pH unit below the IEP of PrP 27-30, well in accordance with other reverse micellar systems; and 4) dynamic light scattering revealed the presence of water-filled reverse micelles in the solubilization controls and a mixed population of protein- and water-filled reverse micelles when PrP 27-30 was used.

Limitations of spectroscopy

FTIR spectroscopy of solubilized PrP 27-30 showed that in most cases, the β-sheet content had not been reduced despite the use of an α-helix-promoting solvent such as TFIP (Gasset et al., 1993; Wille et al., 1996). We initially expected that TFIP might solubilize PrP 27-30 because we had previously shown that it partially disperses prion rods by reducing the β-sheet content without affecting scrapie infectivity. Those studies were done in the presence of 50% sucrose (Wille et al., 1996). The FTIR spectroscopy results we obtained when using 15% TFIP + 1% AOT + 25% sucrose clearly show it was the sucrose that enabled TFIP to promote α-helical structure, presumably by increasing the solvent polarity to such an extent that TFIP interacted with PrP 27-30 more strongly than without sucrose. However, AOT reverse micelles have been demonstrated to decrease the amount of secondary and tertiary structure by favoring extended conformations in proteins such as α-chymotrypsin and cytochrome C (Adachi and Harada, 1994; Qinglong et al., 1994). A similar tendency could protect the β-sheet structure in PrP 27-30 against the influences of TFIP.

Crystallization of PrP 27-30

The crystallization of membrane and membrane-associated proteins is generally difficult, but membrane proteins have a high propensity to form two-dimensional crystals by lateral association inside the lipophilic milieu of natural and synthetic membranes. Factors influencing the crystallization processes in two and three dimensions have been studied in great detail (for reviews see Dolder et al., 1996; Glaeser and Downing, 1993; Michel, 1991).

The crystallization of solubilized PrP 27-30 depended on the use of uranyl salts as a crystallization reagent. AOT reverse micelles have a high propensity to bind monovalent, divalent, and trivalent metal ions effecting a decreased micelle size with increasing ionic valence (Sugimura et al., 1992). Uranyl ions, although not included in the study of Sugimura and co-workers, should tightly bind to AOT reverse micelles owing to their doubly negative charge. This would decrease the micellar size and enable PrP 27-30 molecules to make the contacts necessary for crystal formation. Uranyl ions bind more tightly to SDS micelles than other divalent cations (Reiller et al., 1994); a similar behavior could be expected for AOT reverse micelles and might explain why only the uranyl ion allowed crystal growth. Additionally, the unique linear structure of the *f*-block ura-

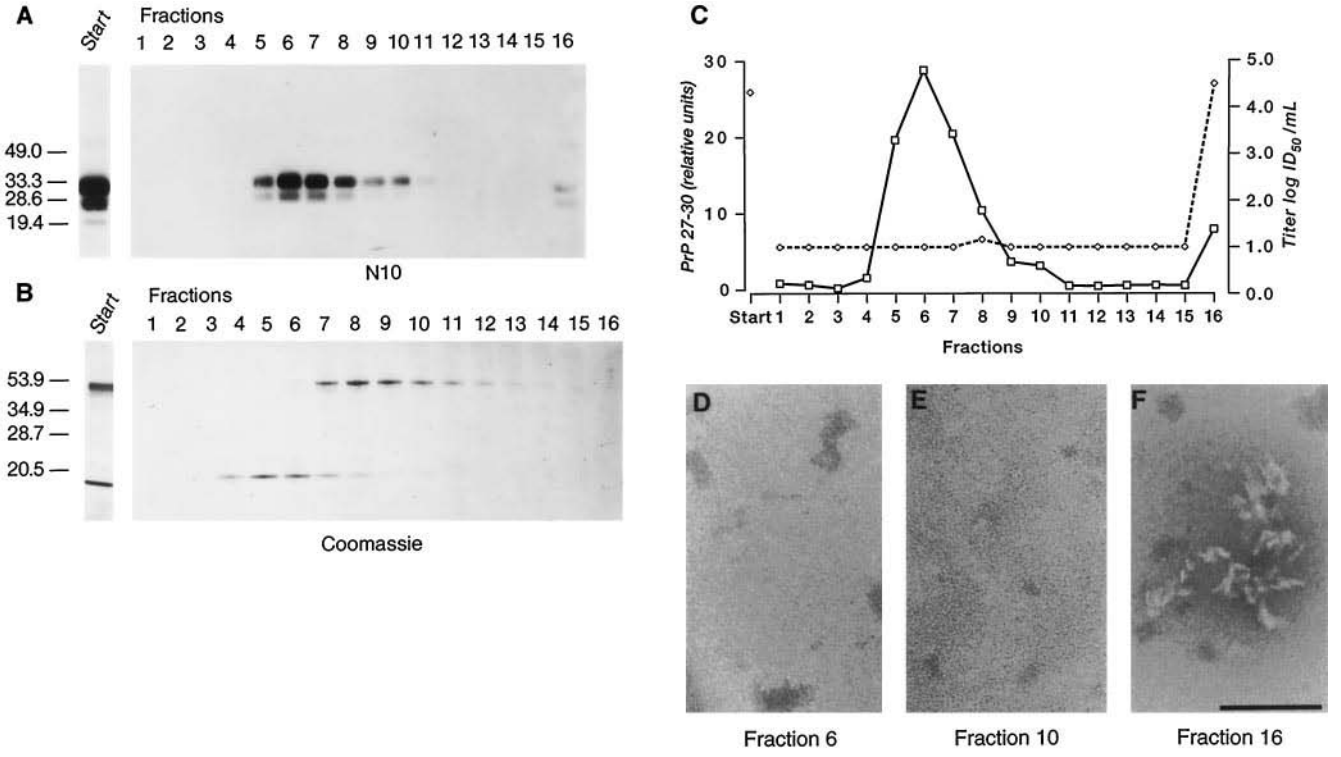

FIGURE 6 Sucrose gradient centrifugation of PrP 27-30 solubilized by 20% TFIP + 1% AOT. (*A*) Solubilized PrP 27-30 was subjected to ultracentrifugation in a 5–20% sucrose gradient. The peak of PrP 27-30 content (fractions 5–8) corresponds to monomeric protein with a $S_{20,w}$ value of ~2 S. A second peak containing less protein (fractions 9–11) corresponds to dimeric PrP 27-30, ~4 S. A relatively faint band of aggregates with >8 S could be seen in the pellet (fraction 16). (*B*) A sample of solubilized PrP 27-30 was mixed with small amounts of ribonuclease A and ovalbumin. A Coomassie-stained SDS PAGE shows the peak of ribonuclease A in fractions 5 and 6 and the peak of ovalbumin in fractions 8 and 9. Sedimentation coefficients for ribonuclease A and ovalbumin from this centrifugation run agree well with published data. The $S_{20,w}$ value of the monomeric PrP 27-30 calculated by comparison to the $S_{20,w}$ values of the ribonuclease A and ovalbumin concurs with the one calculated directly from the sucrose gradient centrifugation. (*C*) Bioassays of the sucrose gradient fractions showed that scrapie infectivity (*dashed line*) could be found only in the pellet fractions containing protein aggregates larger than 8 S, neither PrP 27-30 monomers (fractions 5–8) nor dimers (fractions 8–10) showed significant infectivity. Both curves show the average of three independent experiments. The titer of solubilized PrP 27-30 before the sucrose gradients (*diamond* on the far left) and that of the pellet fraction (number 16) were reasonably similar to infer that all infectivity after solubilization resided in the remaining protein aggregates. All other fractions were below or close to the detection limit of one infectious unit/ml. Negative stain electron microscopy of (*D*) the peak fraction of monomeric PrP 27-30 and (*E*) dimeric PrP 27-30 showed no residual protein aggregates. (*F*) The pellet fraction revealed small aggregates that apparently withstood the solubilization. The appearance of the aggregates is reminiscent of untreated prion rods (compare Fig. 2 *A*). Negative stain 2% ammonium molybdate, bar = 100 nm.

nyl ion makes a replacement by other metal ions seem unlikely.

The role of divalent uranyl ions

A likely explanation for the pH dependency of PrP 27-30 crystallization is the pH-dependent stability of the uranyl ion. At pH 4.0, ~96% of the uranyl ions are present as divalent UO_2^{2+} cations and only ~4% as monovalent $UO_2(OH)^+$; at pH 5.0, UO_2^{2+} is present only at 70% while the $UO_2(OH)^+$ concentration increases to 30% (Moulin et al., 1995). We assume that the monovalent $UO_2(OH)^+$ competes for the binding to the detergent or protein, or possibly both, and thereby inhibits the formation of PrP 27-30 crystals. The observation of unusually strong reflections at 3.1 nm in the electron diffractograms of PrP 27-30 crystallized from 20% isooctane + 2% AOT (Fig. 4 *A*) supports the notion that a complex of PrP 27-30, AOT, and uranyl ions is responsible for the crystallization process. The failure to obtain crystals in the presence of citric acid as a buffer probably stems from the formation of very stable complexes between the uranyl and citrate ions (Abdel Razik et al., 1989), again arguing that uranyl ions are needed to form complexes with PrP 27-30 and the detergent in order for crystals to grow.

Crystallization from a reverse micellar solution

To our knowledge, crystallization of PrP 27-30 from reverse micelles is the first example of the use of such a system to crystallize a membrane protein. Previous work by Wirz and Rosenbusch (1984) mentions attempts to crystallize bacterial porins from reverse micelles, but no reports of successful crystallization followed. A bicontinuous cubic phase, which may be seen as an intermediary between a reverse micellar phase and an aqueous phase with micelles, has

TABLE 4 Secondary structure of PrP 27-30 after treatment with organic solvents, detergents, and combinations

Treatment		Secondary structure (%)			
		α-Helix	β-Sheet	Turns	Coil
PrP 27-30					
in PBSZ*		23	48	9	20
in 25% sucrose*		27	43	13	17
in 25% sucrose + 10% TFIP*		40	28	12	20
Solubilization					
PrP 27-30					
+ buffer only (control)	pellet	24	41	9	26
+ 1% AOT	pellet	26	44	14	16
+ 1% APFO	pellet	14	55	25	6
+ 1% saponin	pellet	17	57	5	21
+ 20% TFIP	pellet#	22	54	7	17
+ 20% TFIP	mixture	30	40	10	20
+ 10% HFPIP	pellet#	21	48	7	24
+ 10% HFPIP	mixture	38	32	10	20
+ 20% isooctane	mixture	26	46	7	21
+ 20% TFIP, 1% AOT	supernatant 2	18	52	7	23
+ 15% TFIP, 1% AOT, 12.5% sucrose	supernatant 2	40	25	13	22
+ 15% TFIP, 1% saponin	supernatant 2	22	51	10	17
+ 20% isooctane, 2% AOT	supernatant 1	24	54	8	14

*Data taken from Wille et al. (1996).
#Actually a mixture of pellet and supernatant 2.

recently been shown to allow three-dimensional crystallization of bacteriorhodopsin (Landau and Rosenbusch, 1996; Pebay-Peyroula et al., 1997). The crystallization of PrP 27-30 may occur through the formation of a bicontinuous cubic phase during the treatment with uranyl salts (but in our case from a reverse micellar system) or may be the result of a reextraction of PrP 27-30 from reverse micelles. AOT complexes with other divalent cations such as cadmium, cobalt, or copper show multiple phases, one being bicontinuous (Petit et al., 1991). A different set of mono and divalent cations such as lithium, beryllium, and magnesium was found to inhibit the formation of AOT reverse micelles (Rabie and Vera, 1997). To our knowledge, no studies of AOT with uranyl ions have been published, leaving the question about the underlying mechanism open to speculation. In either case, it remains to be established whether the crystals we obtained will be suitable for high-resolution diffraction studies. The principal observation that membrane protein crystals can be grown from a reverse micellar solution may prove to be applicable for the crystallization of other membrane proteins.

The nature of the crystallization method and the multiphasic behavior of detergents such as AOT, especially at reduced water contents, increases the possibility of artifacts, which is a potential problem. An AOT bicontinuous cubic phase showed periodicities in x-ray diffractograms of 2.8 nm, 2.5 nm, 1.9 nm, etc.; the hexagonal phase gives reflections that begin at 2.4–3 nm, depending on water content (Ekwall et al., 1970). These diffractograms were obtained from pure AOT; the addition of cations other than Na^+ (particularly multivalent cations) should reduce the lattice spacings by shielding the charges on the AOT molecules similar to what is seen in the liquid reverse micellar state (Petit et al., 1991). Since our lattice spacings are 4 nm for the two-dimensional crystals and 3.7 nm for the hexagonal arrays, this leaves enough room for PrP 27-30 to be included in the crystalline array. Uranyl acetate and two unrelated detergents (sodium 4-(1′-heptylnonyl)benzenesulfonate and sodium octanoate) give crystalline aggregates with a lamellar character and corresponding one-dimensional electron diffraction patterns (Kilpatrick et al., 1985). Uranyl acetate negative stains on AOT and Li^+-AOT showed only micelles and liposome-like structures; no crystalline arrays were observed (Karaman et al., 1994). From these studies and our own efforts to obtain crystalline aggregates from uranyl acetate and AOT alone with or without the presence of TFIP or isooctane, we conclude that the observed crystals are most likely cocrystals of PrP 27-30, AOT, and uranyl ions.

CONCLUDING REMARKS

The solubilization of PrP 27-30 into a reverse micellar solution produces monomeric and dimeric PrP that forms small two- and three-dimensional crystals. Why do the monomers and dimers not possess scrapie infectivity? One possibility is that the monomer and dimer formation was accompanied by partial denaturation, and thus conditions for solubilization of biologic activity still need to be identified. This contention is supported by studies on other proteins noted above, where AOT reverse micelles decreased the amount of secondary and tertiary structure favoring extended conformations of the proteins (Adachi and Harada, 1994; Qinglong et al., 1994). Another possibility is

that monomers and dimers are more readily cleared from the CNS after inoculation than are large aggregates, which are more protected from degradation by tissue proteases (Prusiner et al., 1998; Safar et al., 1998).

To our knowledge, this is the first description of crystals of a β-sheet-rich PrP derived from PrP 27-30; moreover, it may be the first demonstration of the crystallization of a membrane or membrane-associated protein directly from a reverse micellar system. The PrP crystals appear to be suitable for structural analysis by electron crystallography. Indeed, if larger three-dimensional crystals of PrP 27-30 can be formed, then it may be possible to determine the structure of the protein by x-ray crystallography.

We thank Drs. Fred E. Cohen, Jiri Safar, Robert M. Stroud, David A. Agard, and Vincent Guénebaut for many helpful discussions, Hana Serban and her colleagues for preparation of PrP 27-30, Dr. Marilyn Torchia for the bioassays, and Mei-Lie Wong for making darkroom facilities available.

This work was supported by National Institutes of Health Grants NS14069, AG08967, AG02132, and NS22786, the International Human Frontiers of Science Program, and the American Health Assistance Foundation, as well as by gifts from the Sherman Fairchild Foundation, the G. Harold and Leila Y. Mathers Foundation, the Bernard Osher Foundation, and Centeon.

REFERENCES

Abdel Razik, A., F. A. Ali, and F. Abu Attia. 1989. Evaluation of the stability constants of uranyl association complexes with phosphate, oxalate, tartrate, and citrate anions in solutions of constant ionic strength. *Microchem. J.* 39:265–269.

Adachi, M., and M. Harada. 1994. Time dependence of the solubilization state of cytochrome c in AOT water-in-oil microemulsion. *J. Colloid Interface Sci.* 165:229–235.

Akowitz, A., T. Sklaviadis, E. E. Manuelidis, and L. Manuelidis. 1990. Nuclease-resistant polyadenylated RNAs of significant size are detected by PCR in highly purified Creutzfeldt-Jakob disease preparations. *Microb. Pathog.* 9:33–45.

Bessen, R. A., and R. F. Marsh. 1994. Distinct PrP properties suggest the molecular basis of strain variation in transmissible mink encephalopathy. *J. Virol.* 68:7859–7868.

Bolton, D. C., M. P. McKinley, and S. B. Prusiner. 1982. Identification of a protein that purifies with the scrapie prion. *Science*. 218:1309–1311.

Bomford, R., M. Stapleton, S. Winsor, J. E. Beesley, E. A. Jessup, K. R. Price, and G. R. Fenwick. 1992. Adjuvanticity and ISCOM formation by structurally diverse saponins. *Vaccine*. 10:572–577.

Byler, D. M., and H. Susi. 1986. Examination of the secondary structure of proteins by deconvolved FTIR spectra. *Biopolymers*. 25:469–487.

Caughey, B., and B. Chesebro. 1997. Prion protein and the transmissible spongiform encephalopathies. *Trends Cell Biol.* 7:56–62.

Caughey, B. W., A. Dong, K. S. Bhat, D. Ernst, S. F. Hayes, and W. S. Caughey. 1991. Secondary structure analysis of the scrapie-associated protein PrP 27-30 in water by infrared spectroscopy. *Biochemistry*. 30:7672–7680.

Caughey, B., G. J. Raymond, D. A. Kocisko, and P. T. Lansbury, Jr. 1997. Scrapie infectivity correlates with converting activity, protease resistance, and aggregation of scrapie-associated prion protein in guanidine denaturation studies. *J. Virol.* 71:4107–4110.

Cohen, F. E., and S. B. Prusiner. 1998. Pathologic conformations of prion proteins. *Annu. Rev. Biochem.* 67:793–819.

Dolder, M., A. Engel, and M. Zulauf. 1996. The micelle to vesicle transition of lipids and detergents in the presence of a membrane protein: towards a rationale for 2D crystallization. *FEBS Lett.* 382:203–208.

Durchschlag, H. 1986. Specific volumes of biological macromolecules and some other molecules of biological interest. *In* Thermodynamic Data for Biochemistry and Biotechnology. H.-J. Hinz, editor. Springer-Verlag, Berlin. 45–128.

Eigen, M. 1996. Prionics or the kinetic basis of prion diseases. *Biophys. Chem.* 63:A11–A18.

Ekwall, P., L. Mandell, and K. Fontell. 1970. Some observations on binary and ternary aerosol OT systems. *J. Colloid Interface Sci.* 33:215–235.

Endo, T., D. Groth, S. B. Prusiner, and A. Kobata. 1989. Diversity of oligosaccharide structures linked to asparagines of the scrapie prion protein. *Biochemistry*. 28:8380–8388.

Fletcher, P. D. I., N. M. Perrins, B. H. Robinson, and C. Toprakcioglu. 1982. Purity of aerosol-OT (AOT): effect on processes in reversed micelles and water-in-oil microemulsions. *In* Reverse Micelles. P. L. Luisi and B. E. Straub, editors. Plenum Press, New York. 69–72.

Gabizon, R., M. P. McKinley, and S. B. Prusiner. 1987. Purified prion proteins and scrapie infectivity copartition into liposomes. *Proc. Natl. Acad. Sci. USA*. 84:4017–4021.

Gabizon, R., M. P. McKinley, and S. B. Prusiner. 1988. Properties of scrapie prion proteins in liposomes and amyloid rods. *In* Novel Infectious Agents and the Central Nervous System, Ciba Foundation Symposium 135. G. Bock and J. Marsh, editors. John Wiley & Sons, Chichester, UK. 182–196.

Gajdusek, D. C. 1988. Transmissible and non-transmissible amyloidoses: autocatalytic post-translational conversion of host precursor proteins to β-pleated sheet configurations. *J. Neuroimmunol.* 20:95–110.

Gasset, M., M. A. Baldwin, R. J. Fletterick, and S. B. Prusiner. 1993. Perturbation of the secondary structure of the scrapie prion protein under conditions that alter infectivity. *Proc. Natl. Acad. Sci. USA*. 90:1–5.

Glaeser, R. M., and K. H. Downing. 1993. High-resolution electron crystallography of protein molecules. *Ultramicroscopy*. 52:478–486.

Göklen, K. E., and T. A. Hatton. 1987. Liquid-liquid extraction of low molecular-weight proteins by selective solubilization in reversed micelles. *Sep. Sci. Technol.* 22:831–841.

Harper, J. D., and P. T. Lansbury, Jr. 1997. Models of amyloid seeding in Alzheimer's disease and scrapie: mechanistic truths and physiological consequences of the time-dependent solubility of amyloid proteins. *Annu. Rev. Biochem.* 66:

Harrison, P. M., P. Bamborough, V. Daggett, S. B. Prusiner, and F. E. Cohen. 1997. The prion folding problem. *Curr. Opin. Struct. Biol.* 7:53–59.

Hsiao, K. K., D. Groth, M. Scott, S.-L. Yang, H. Serban, D. Rapp, D. Foster, M. Torchia, S. J. DeArmond, and S. B. Prusiner. 1994. Serial transmission in rodents of neurodegeneration from transgenic mice expressing mutant prion protein. *Proc. Natl. Acad. Sci. USA*. 91: 9126–9130.

Hunter, G. D., R. H. Kimberlin, and R. A. Gibbons. 1968. Scrapie: a modified membrane hypothesis. *J. Theor. Biol.* 20:355–357.

Hunter, G. D., and G. C. Millson. 1967. Attempts to release the scrapie agent from tissue debris. *J. Comp. Pathol.* 77:301–307.

Jarrett, J. T., and P. T. Lansbury, Jr. 1993. Seeding "one-dimensional crystallization" of amyloid: a pathogenic mechanism in Alzheimer's disease and scrapie? *Cell.* 73:1055–1058.

Karaman, M. E., B. W. Ninham, and R. M. Pashley. 1994. Some aqueous solution and surface properties of dialkyl sulfosuccinate surfactants. *J. Phys. Chem.* 98:11512–11518.

Kersten, G. F. A., A. Spiekstra, E. C. Beuvery, and D. J. A. Crommelin. 1991. On the structure of immune-stimulating saponin-lipid complexes (iscoms). *Biochim. Biophys. Acta*. 1062:165–171.

Kilpatrick, P. K., W. G. Miller, and Y. Talmon. 1985. Staining and drying-induced artifacts in electron microscopy of surfactant dispersions. II. Change in phase behavior produced by variation in pH modifiers, stain, and concentration. *J. Colloid Interface Sci.* 107:146–158.

Kimberlin, R. H., G. C. Millson, and G. D. Hunter. 1971. An experimental examination of the scrapie agent in cell membrane mixtures. III. Studies of the operational size. *J. Comp. Pathol.* 81:383–391.

Landau, E. M., and J. P. Rosenbusch. 1996. Lipidic cubic phases: a novel concept for the crystallization of membrane proteins. *Proc. Natl. Acad. Sci. USA*. 93:14532–14535.

Malone, T. G., R. F. Marsh, R. P. Hanson, and J. S. Semancik. 1978. Membrane-free scrapie activity. *J. Virol.* 25:933–935.

Marsh, R. F., C. Dees, B. E. Castle, W. F. Wade, and T. L. German. 1984. Purification of the scrapie agent by density gradient centrifugation. *J. Gen. Virol.* 65:415–421.

McKinley, M. P., R. K. Meyer, L. Kenaga, F. Rahbar, R. Cotter, A. Serban, and S. B. Prusiner. 1991. Scrapie prion rod formation in vitro requires both detergent extraction and limited proteolysis. *J. Virol.* 65: 1340–1351.

Michel, H. 1991. Crystallization of Membrane Proteins. CRC Press, Boca Raton, FL.

Millson, G., G. D. Hunter, and R. H. Kimberlin. 1971. An experimental examination of the scrapie agent in cell membrane mixtures. II. The association of scrapie infectivity with membrane fractions. *J. Comp. Pathol.* 81:255–265.

Millson, G. C., G. D. Hunter, and R. H. Kimberlin. 1976. The physicochemical nature of the scrapie agent. *In* Slow Virus Diseases of Animals and Man. R. H. Kimberlin, editor. American Elsevier, New York. 243–266.

Moulin, C., P. Decambox, V. Moulin, and J. G. Decaillon. 1995. Uranium speciation in solution by time-resolved laser-induced fluorescence. *Anal. Chem.* 67:348–353.

Pan, K.-M., M. Baldwin, J. Nguyen, M. Gasset, A. Serban, D. Groth, I. Mehlhorn, Z. Huang, R. J. Fletterick, F. E. Cohen, and S. B. Prusiner. 1993. Conversion of α-helices into β-sheets features in the formation of the scrapie prion proteins. *Proc. Natl. Acad. Sci. USA*. 90:10962–10966.

Pebay-Peyroula, E., G. Rummel, J. P. Rosenbusch, and E. M. Landau. 1997. X-ray structure of bacteriorhodopsin at 2.5 angstroms from microcrystals grown in lipidic cubic phases. *Science*. 277:1676–1681.

Petit, C., P. Lixon, and M. P. Pileni. 1991. Structural study of bimetallic bis(2-ethylhexyl) sulfosuccinate aggregates. *Langmuir*. 7:2620–2625.

Prusiner, S. B. 1997. Prion diseases and the BSE crisis. *Science*. 278: 245–251.

Prusiner, S. B., D. C. Bolton, D. F. Groth, K. A. Bowman, S. P. Cochran, and M. P. McKinley. 1982. Further purification and characterization of scrapie prions. *Biochemistry*. 21:6942–6950.

Prusiner, S. B., D. F. Groth, S. P. Cochran, F. R. Masiarz, M. P. McKinley, and H. M. Martinez. 1980. Molecular properties, partial purification, and assay by incubation period measurements of the hamster scrapie agent. *Biochemistry*. 19:4883–4891.

Prusiner, S. B., W. J. Hadlow, D. E. Garfin, S. P. Cochran, J. R. Baringer, R. E. Race, and C. M. Eklund. 1978. Partial purification and evidence for multiple molecular forms of the scrapie agent. *Biochemistry*. 17: 4993–4997.

Prusiner, S. B., M. P. McKinley, K. A. Bowman, D. C. Bolton, P. E. Bendheim, D. F. Groth, and G. G. Glenner. 1983. Scrapie prions aggregate to form amyloid-like birefringent rods. *Cell*. 35:349–358.

Prusiner, S. B., M. R. Scott, S. J. DeArmond, and F. E. Cohen. 1998. Prion protein biology. *Cell*. 93:337–348.

Prusiner, S. B., M. Scott, D. Foster, K.-M. Pan, D. Groth, C. Mirenda, M. Torchia, S.-L. Yang, D. Serban, G. A. Carlson, P. C. Hoppe, D. Westaway, and S. J. DeArmond. 1990. Transgenetic studies implicate interactions between homologous PrP isoforms in scrapie prion replication. *Cell*. 63:673–686.

Qinglong, C., L. Huizhou, and C. Jiayong. 1994. Fourier transform infrared spectra studies of protein in reverse micelles: effect of AOT/isooctane on the secondary structure of α-chymotrypsin. *Biochim. Biophys. Acta.* 1206:247–252.

Rabie, H. R., D. Helou, M. E. Weber, and J. H. Vera. 1997. Comparison of the titration and contact methods for the water solubilization capacity of AOT reverse micelles in the presence of a cosurfactant. *J. Colloid Interface Sci.* 189:208–215.

Rabie, H. R., and J. H. Vera. 1997. Counterion binding to ionic reverse micellar aggregates and its effect on water uptake. *J. Phys. Chem. B*. 101:10295–10302.

Reiller, P., D. Lemordant, C. Moulin, and C. Beaucaire. 1994. Dual use of micellar-enhanced ultrafiltration and time-resolved laser-induced spectrofluorimetry for the study of uranyl exchange at the surface of alkylsulfate micelles. *J. Colloid Interface Sci.* 163:81–86.

Riesner, D., K. Kellings, K. Post, H. Wille, H. Serban, D. Groth, M. A. Baldwin, and S. B. Prusiner. 1996. Disruption of prion rods generates 10-nm spherical particles having high α-helical content and lacking scrapie infectivity. *J. Virol.* 70:1714–1722.

Safar, J. 1996. The folding intermediate concept of prion protein formation and conformational links to infectivity. *In* Prions Prions Prions. S. B. Prusiner, editor. Springer-Verlag, Heidelberg. 69–76.

Safar, J., M. Ceroni, D. C. Gajdusek, and C. J. Gibbs, Jr. 1991. Differences in the membrane interaction of scrapie amyloid precursor proteins in normal and scrapie- or Creutzfeldt-Jakob disease-infected brains. *J. Infect. Dis.* 163:488–494.

Safar, J., P. P. Roller, D. C. Gajdusek, and C. J. Gibbs, Jr. 1993. Conformational transitions, dissociation, and unfolding of scrapie amyloid (prion) protein. *J. Biol. Chem.* 268:20276–20284.

Safar, J., H. Wille, V. Itri, D. Groth, H. Serban, M. Torchia, F. E. Cohen, and S. B. Prusiner. 1998. Eight prion strains have PrP^{Sc} molecules with different conformations. *Nat. Med.* 4:1157–1165.

Semancik, J. S., R. F. Marsh, J. L. Geelen, and R. P. Hanson. 1976. Properties of the scrapie agent-endomembrane complex from hamster brain. *J. Virol.* 18:693–700.

Sklaviadis, T., R. Dreyer, and L. Manuelidis. 1992. Analysis of Creutzfeldt-Jakob disease infectious fractions by gel permeation chromatography and sedimentation field flow fractionation. *Virus Res.* 26: 241–254.

Stahl, N., M. A. Baldwin, R. Hecker, K.-M. Pan, A. L. Burlingame, and S. B. Prusiner. 1992. Glycosylinositol phospholipid anchors of the scrapie and cellular prion proteins contain sialic acid. *Biochemistry*. 31:5043–5053.

Steensgaard, J., S. Humphries, and S. P. Spragg. 1992. Measurements of sedimentation coefficients. *In* Preparative Centrifugation: A Practical Approach. D. Rickwood, editor. IRL Press, Oxford. 187–232.

Steensgaard, J., N. P. H. Møller, and L. Funding. 1978. Rate-zonal centrifugation: quantitative aspects. *In* Centrifugal Separations in Molecular and Cell Biology. G. D. Birnie and D. Rickwood, editors. Butterworths, London. 115–163.

Sugimura, T., Y. Sindo, M. Hasegawa, A. Kitahara, and Y. Masuda. 1992. Preparation of AOT-metal surfactants and their properties in nonaqueous and aqueous media. *J. Dispersion Sci. Technol.* 13:251–269.

Telling, G. C., T. Haga, M. Torchia, P. Tremblay, S. J. DeArmond, and S. B. Prusiner. 1996a. Interactions between wild-type and mutant prion proteins modulate neurodegeneration in transgenic mice. *Genes Dev.* 10:1736–1750.

Telling, G. C., P. Parchi, S. J. DeArmond, P. Cortelli, P. Montagna, R. Gabizon, J. Mastrianni, E. Lugaresi, P. Gambetti, and S. B. Prusiner. 1996b. Evidence for the conformation of the pathologic isoform of the prion protein enciphering and propagating prion diversity. *Science*. 274:2079–2082.

Timmermans, J. 1950. Physico-chemical Constants of Pure Organic Compounds. Elsevier Publishing Company, Inc., New York.

Wille, H., G.-F. Zhang, M. A. Baldwin, F. E. Cohen, and S. B. Prusiner. 1996. Separation of scrapie prion infectivity from PrP amyloid polymers. *J. Mol. Biol.* 259:608–621.

Wirz, J., and J. P. Rosenbusch. 1984. The formation of reverse mixed micelles consisting of membrane proteins and AOT in isooctane. *In* Reverse Micelles. P. L. Luisi and B. E. Straub, editors. Plenum Press, New York. 231–238.

Wolbert, R. B. G., R. Hilhorst, G. Voskuilen, H. Nachtegaal, M. Dekker, K. Van't Riet, and B. H. Bijsterbosch. 1989. Protein transfer from an aqueous phase into reversed micelles. The effect of protein size and charge distribution. *Eur. J. Biochem.* 184:

Zampieri, G. G., H. Jäckle, and P. L. Luisi. 1986. Determination of the structural parameters of reverse micelles after uptake of proteins. *J. Phys. Chem.* 90:1849–1853.